

## Source parameter estimates for some historical earthquakes in the south-eastern Alps using ground shaking scenarios

L. TIBERI, G. COSTA and P. SUHADOLC

*Dipartimento di Matematica e Geoscienze, Università di Trieste, Italy*

(Received: June 13, 2013; accepted: February 20, 2014)

**ABSTRACT** Some of the most relevant seismogenic sources in north-eastern Italy, western Slovenia and southern Austria have been studied in the framework of the Interreg IV A HAREIA (Historical And Recent Earthquakes in Italy and in Austria) project. Based on active fault data and historical records we have produced several ground shaking scenarios for some of the biggest known historical earthquakes that have occurred in the studied area. In particular, we compute the maximum peak ground velocity value at 1 Hz ( $PGVIH_z$ ) for all studied events at every point of the computation grid, which covers the entire area of interest. For each studied earthquake we, then, make a qualitative comparison between the related observed intensity data points and computed scenarios, and select the one that is most consistent. This allows us to determine both the causative fault model and the approximate extended-fault rupturing process at the basis of each earthquake. We have applied this analysis to know historical events such as the Villach (1348), Idrija (1511), Asolo (1695) and Tyrol (1572, 1670, and 1689) earthquakes. We have added to the results obtained from these events several scenarios related to other important events that occurred or we deem possible to occur in the area and for which the causative fault is known. The maximum value obtained from all computed scenarios at a given grid point allows finally the construction of a  $PGVIH_z$  map for the area under investigation. Such a map, a main result of this study, can be used as a conservative seismic hazard one for events that might occur on the considered active faults.

**Key words:** historical earthquakes, shaking scenario, SE Alps.

### 1. Introduction

In the south-eastern Alps destructive earthquakes with magnitudes between 5 and 7 occurred in the past and might therefore occur again in the future. Knowledge about past earthquakes – based on historical research – that occurred in pre-instrumental or early instrumental times is crucial in the assessment of seismic hazard of a given territory, and thus useful also to regional governments and regional planning bodies that have to develop prevention and civil protection plans. The identification and characterization of active faults, as seismogenic sources, plays an equally fundamental role in the field of seismic hazard assessment and can be used to simulate realistic ground motion scenarios, and to mitigate the damages due to future earthquakes.

This is the reason an Austria - Italy Interreg project was carried on in the south-eastern Alps on this theme by the Protezione Civile Regionale (Regional Civil Defense) of Friuli Venezia

Giulia, South Tyrol and Tyrol. The scientific investigations were performed by the Dipartimento di Matematica e Geoscienze (Department of Mathematics and Geosciences) of the University of Trieste (DMG - UTS), the Istituto Nazionale di Oceanografia e di Geofisica Sperimentale (National Institute for Oceanography and Applied Geophysics: OGS), the Istituto Nazionale di Geofisica e Vulcanologia (National Institute of Geophysics and Volcanology: INGV) and the Zentralanstalt für Meteorologie und Geodynamik (Central Office for Meteorology and Geodynamics: ZAMG) in Vienna.

The fault parameters that characterize a potential seismogenic source, used as input for the ground motion scenarios, can be estimated either from the seismotectonic analysis of the source area (e.g., Burrato *et al.*, 2008), or from empirical relationships between fault dimensions and magnitude (e.g., Wells and Coppersmith, 1994). The latter is based on the information contained in historical catalogues produced by INGV, OGS and ZAMG, our collaborators in the project. It is also possible to determine the causative source of a historical event by comparing its estimated intensity data-points with the maximum amplitude of ground velocity, computed via synthetic seismograms and a source model (scenario event) at the same locations (e.g., Fitzko *et al.*, 2005). For some events the estimated intensity data-points have been proposed or computed as new by our project partners.

Initially, we have tested our method on the Bovec (Slovenia) 1998 event. In this case synthetic seismograms have been calculated not only on a pre-determined grid but also at some existing stations that have recorded the related ground motion in order to compare the fit between real and synthetic seismograms (Bajc *et al.*, 2001). Afterwards, we have calculated three different scenarios in terms of the maximum peak ground velocity value at 1Hz ( $PGV1Hz$ ) for the Bovec 1998 event in order to calibrate the method (Moratto *et al.*, 2009) in our area of interest.

During the HAREIA project we have analyzed the Villach 1348, Idrija 1511, Asolo 1695 and Tyrol 1572, 1670 and 1689 events. The calculated  $PGV1Hz$  values are qualitatively compared with the intensity data-points, in order to identify the causative source. We have added to the results obtained from the events studied in the framework of the project several scenarios related to other important events that occurred or we deem possible to occur in the area. For each event the maximum value of  $PGV1Hz$  for all considered scenarios at every point of the grid has been considered. Our final product is then a maximized scenario map in terms of  $PGV1Hz$ , calculated on the basis of all scenarios for all the analyzed events (both HAREIA and other events) at each point of a grid covering our area of interest (Fig. 1). Such a map can be used as a conservative seismic hazard one for events that might occur on the considered active faults and can provide some useful, albeit very preliminary and subject to limitations, information to regional governments in order to update their prevention plans and to reduce the consequences of hypothetical future earthquakes.

## 2. Ground motion simulation techniques

All the shaking scenarios are calculated using an extended-fault model, applying a constant model of velocity of rupture propagation, and varying the epicentre position along the fault. The assumed distribution of seismic moment is either homogeneous or non-uniform. In this way, for every fault model, also using different possible fault rupture mechanisms, we have calculated

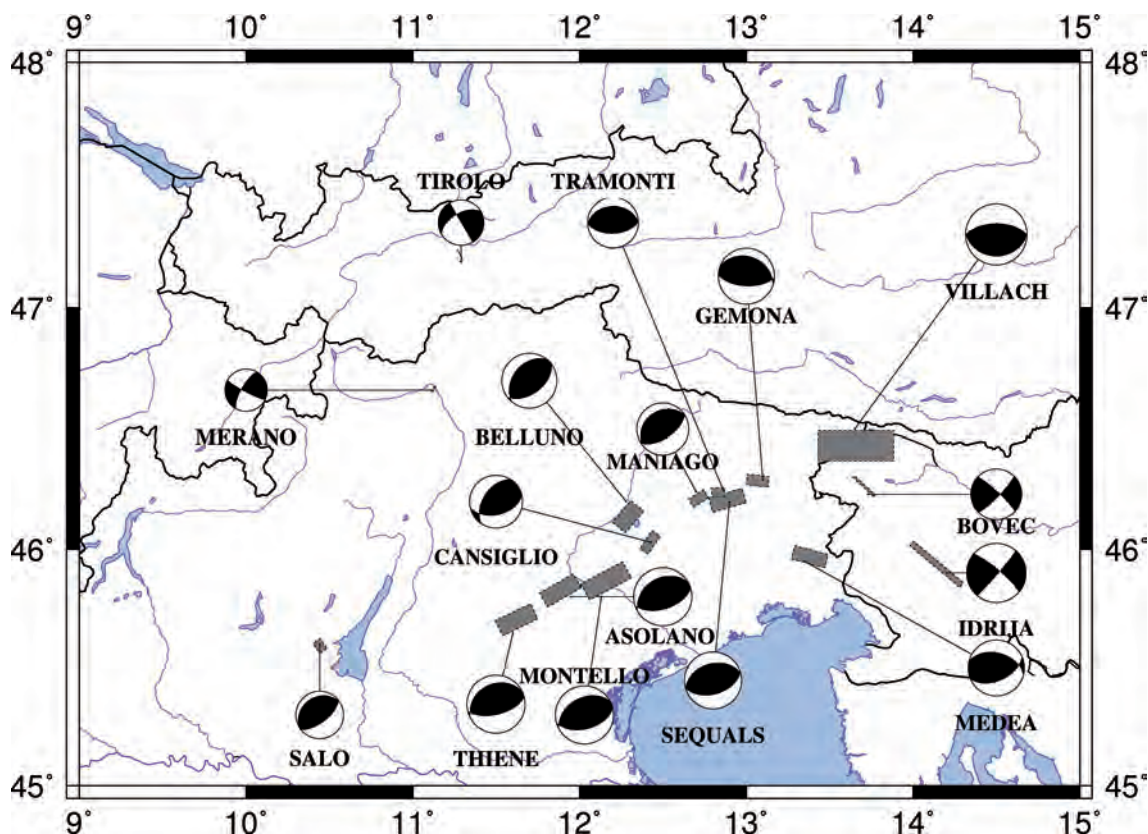


Fig. 1 - Map reporting all the studied events in this work during HAREIA project and the ones analyzed in order to cover the entire area of interest.

several shaking scenarios. The synthetic seismograms (Fig. 2), calculated using the multimodal summation approach (Panza and Suhadolc, 1987; Florsch *et al.*, 1991), are computed with a maximum frequency of 1 Hz on each point of a dense equidistant receivers grid. From every receiver we can obtain the maximum value of acceleration, velocity or displacement.

The calculation of synthetic seismograms requires the knowledge of both source parameters and a structural model (velocities, layer thicknesses and anelasticity values). The choice of the maximum frequency used is crucial, because ground motion parameters must be estimated within a frequency range as large as possible. At high frequencies, however, seismograms are strongly influenced by the short-wavelength complexities of the medium. In this paper seismograms are therefore calculated at a maximum frequency of 1 Hz using the 1D velocity model “est4a” proposed by Costa *et al.* (1992), appropriate for this particular region of the southern Alps. This 1D velocity model is sufficient for 1 Hz computations, also because the structure at smaller wavelengths is not known. Another limit of this method are the site effects, which have not been considered in this study. Site effects can certainly affect the intensity, usually by half or one intensity value. This uncertainty is under our level of precision in our qualitative comparison, so it does not influence our results.

Ground motion scenarios are calculated using a kinematic approach for extended sources (e.g., Saraò *et al.*, 1998). The extended-fault model requires, as input, the parameters that

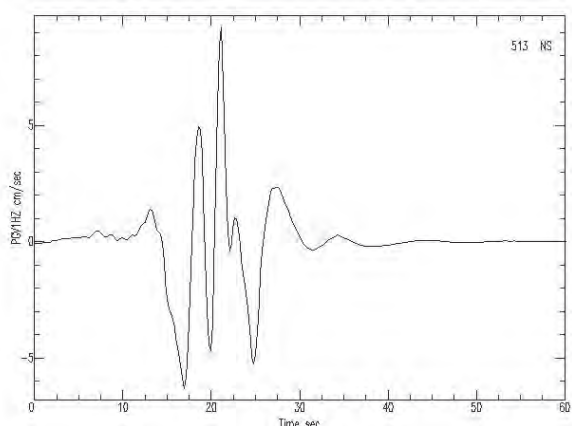


Fig. 2 - An example of a synthetic seismogram, east component, calculated for the Villach event of 1348.

describe the source geometry and the rupture process along the fault. The rupture surface is assumed to be a rectangle, described by a length,  $L$ , and a width,  $W$ , usually correlated with the seismic moment (e.g., Wells and Coppersmith, 1994).

The fracture process is described by a distribution of slip or seismic moment, function of time and of coordinates along the fault plane. We assume an *a-priori* distribution of the seismic moment. The simplest distribution is a constant one on the fault surface and tapered to zero at the borders. A more realistic approach, also used in our computations, considers the seismic moment concentrated to restricted areas of the fault, called asperities, where the slip vector is statistically 1.5 higher than its average value (Somerville *et al.*, 1999). The asperities (Fig. 3) are modeled using the  $k^2$  law (Herrero and Bernard, 1994).

The time dependence of seismic moment (or slip) is described by a propagation model of the rupture which requires a fixed position of the nucleation point on the fault, a fixed rupture propagation velocity  $v_r$ , usually taken as  $0.72 \beta$  with  $\beta$  the S-wave velocity in the medium, and a characteristic rise time for each point of the source (Heaton, 1990). In the extended-fault

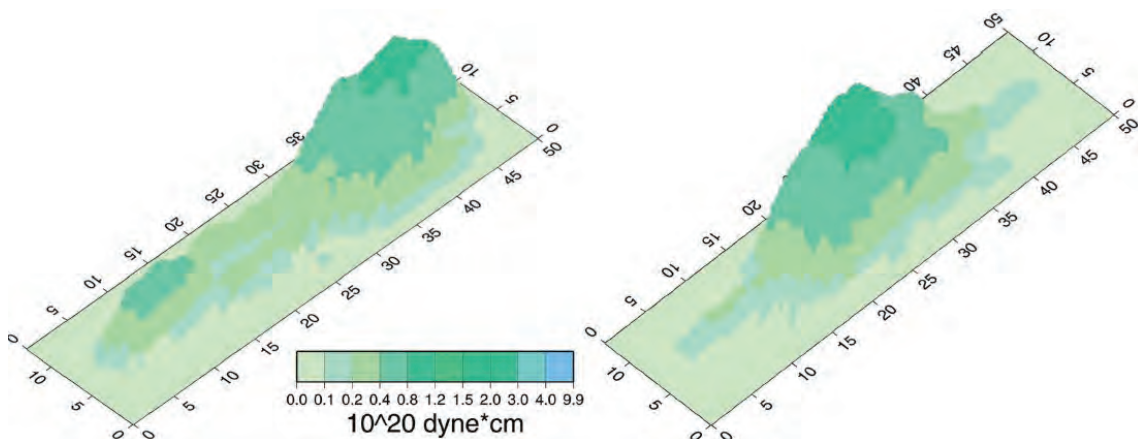


Fig. 3 - Two examples of seismic moment distribution with one and two asperities.

model, synthetic seismograms at a given receiver are calculated as the summation of all the contributions of every single cell in which the rupture surface has been discretized.

The locations of the analyzed historical earthquakes in this work are taken from suggestions provided by our project partners: INGV, OGS and ZAMG. Based on fault dimensions obtained from Wells and Coppersmith (1994) relationships, and considering three possible nucleation points (both ends and centre of the fault) in order to include directivity effects in case of a bilateral or unilateral rupture, we have computed several ground motion scenarios. In the case of events with moment magnitude greater than 5.5, we have chosen also both a double- and a one-asperity seismic moment distribution.

For the HAREIA events, we make also a qualitative comparison between our computed  $PGVIHz$  values and the intensity values obtained from pre-existing databases, such as the Italian earthquake parameter catalogue from now on referred to as CPTI11 (Rovida *et al.*, 2011), and from intensity data collected or estimated during this project by our partners, e.g., ZAMG for the three Tyrol events (Hammerl *et al.*, 2012).

All shaking scenarios in this paper are calculated, as already mentioned, with a maximum frequency of 1 Hz, both in the case of peak ground accelerations ( $PGA1Hz$ ) and for the peak ground velocities ( $PGVIHz$ ). In this work we consider only the  $PGVIHz$  values because velocity is more related to damage for earthquakes in the considered magnitude range. The reason for preferring  $PGVIHz$  to  $PGA1Hz$  is well explained in Wald *et al.* (2005), since for the great majority of considered events the intensities are VII and above and since the correlation with intensity and  $PGV$  can be considered to be significant at 1 Hz. Intensity and velocity values are not directly comparable unless we convert velocity values into “instrumental” intensities. Such relationships are affected by large uncertainties and, in addition, such empirical relationships are not available for data having the maximum frequency value at 1 Hz. For these reasons we have qualitatively compared only the pattern of the intensity data-points and the related peak velocity distributions.

### 3. Ground motion scenarios

Following a chronological order from historical to recent, we describe in the following the four seismogenic sources analyzed during HAREIA project and the related ground motion shaking scenarios calculated for each of these. Here, in Table 1 we have summarized the source parameters of all the events studied within the HAREIA project. For Tyrol events, we do not have an indication of where the possible epicentre was located, so we have analyzed a few faults in the area and we have modeled all of them.

#### 3.1. Villach 1348 event

The Villach event, occurred on January 25, 1348, was assumed to be located near the city of Villach (Austria), after which it is named. Indeed, most of the early studies on this earthquake, locate the epicentral area around Villach on the basis of dramatic effects in the area as described by written sources (e.g., Ambraseys, 1976; Gentile *et al.*, 1985). The 1348 earthquake was later on extensively studied as a case history by Hammerl (1992, 1994). According to her study in which she uses only contemporary sources “heavy damage is concentrated in the Friuli area and



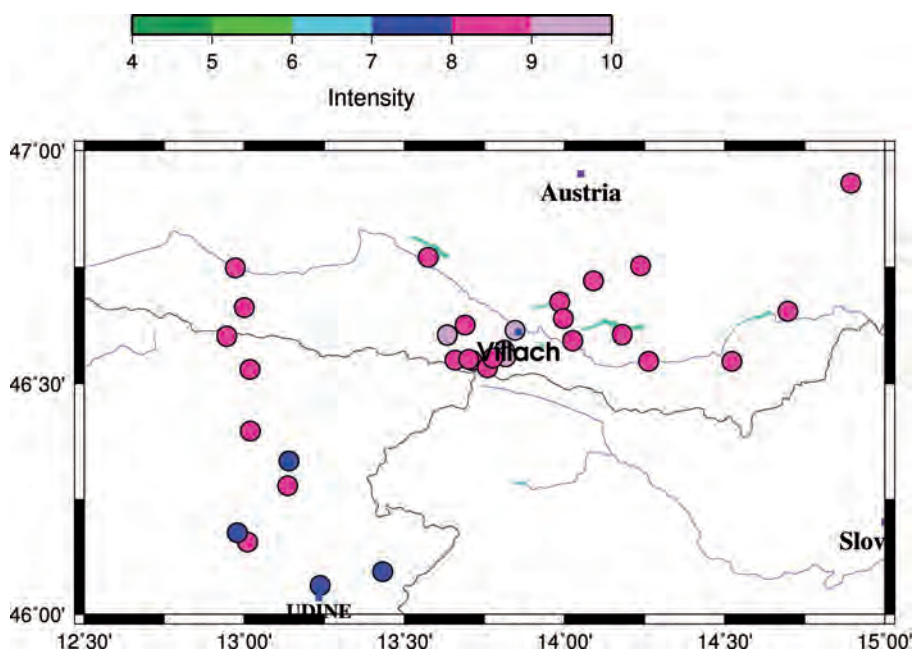


Fig. 5 - Intensity data-points due to the Villach 1348 event (from CPT111).

damage is reported in some localities in the south of Carinthia, the NW of Slovenia and in the NE of Italy” (Fig. 4). Using only these contemporary sources Gutdeutsch and Lenhardt (1996) compare the related intensities with those of the theoretical intensity distribution of the Friuli 1976 event and find that the epicentre is close to the one of the Friuli event (Tarcento area), however the magnitude of the 1348 event had to be stronger or its focal depth deeper. They also note that the damage in the Villach area is not well fitted by their model.

The location of this earthquake is, therefore, still a matter of debate and study for historians. Caracciolo and Camassi (2005), our project partners, propose an epicentre near Val Canale. This hypothesis led us to consider as generating fault for this event, the Fella - Sava thrust fault (Carulli, 2006; Ponton, 2010), that in its eastward extension, known in Slovenia as the Sava fault, has a dominant strike-slip character.

As already mentioned, the 1348 earthquake mostly damaged the area near and to the north of Villach, but caused also remarkable damage in today's Friuli Venezia Giulia (Fig. 5).

Since no focal plane solution has been proposed in the past, we validate some models using available seismotectonic information. In this work, we adopt the epicentre of Caracciolo and Camassi (2005), located at  $46.493^{\circ}$  N,  $13.428^{\circ}$  E. We have chosen the source parameters in agreement with the fault characteristics as deduced from the geological map of Carulli (2006) and from the Ponton profiles (2010), as you can see in Table 1. The complexity of the slip on the fault was reproduced using a double-asperity moment distribution.

### 3.1.1. Bilateral rupture

The ground-shaking scenario for a bilateral rupture with a double-asperity seismic moment distribution (Fig. 6 left side) shows an area of strong shaking in the eastern direction (where the major asperity is located), along the fault strike. The zone, where the maximum of horizontal

velocities are present ( $\sim 80$  cm/s) is located near the eastern edge of the fault. The shaking is, therefore, more prominent towards NE (rupture propagation towards the surface) than in the other directions (see also isoline 40 cm/s). It seems, that this scenario well explains the damage to the north of the fault, especially in Austria, but not very well to the south, in Friuli Venezia Giulia (Caracciolo and Camassi, 2005). On the other hand, the scenario for a bilateral rupture with a uniform seismic moment distribution (Fig. 6, right side) well explains both the damages occurred in Austria and in Friuli Venezia Giulia.

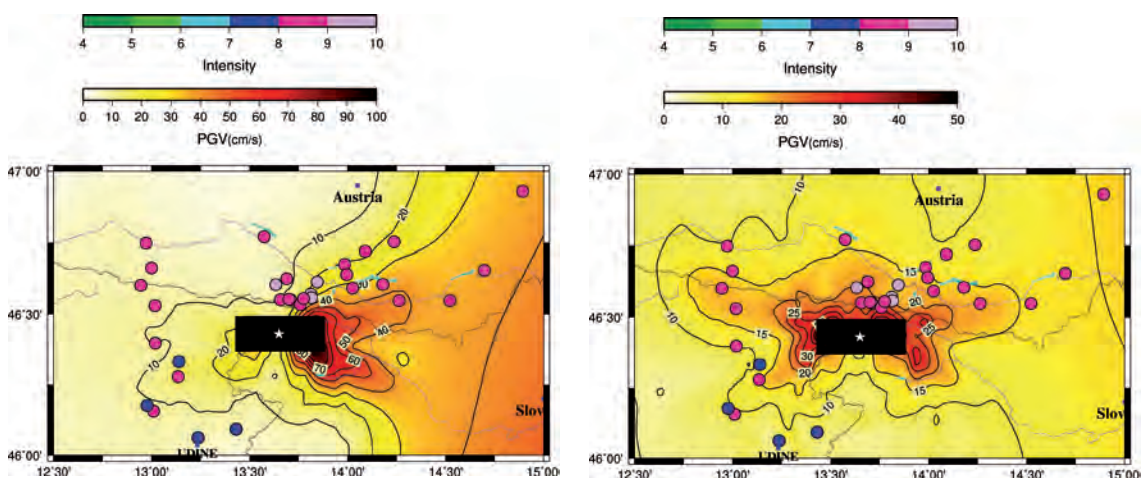


Fig. 6 - Villach 1348 event, bilateral rupture. The scenarios are superimposed on the observed intensity values (from CPT111). The black rectangle and the white star are the surface projections of the fault and of the nucleation point, respectively. Left: scenario with a double-asperity seismic moment distribution. Right: scenario with a uniform seismic moment distribution.

### 3.1.2. Unilateral ruptures

In the next two scenarios (Fig. 7) we have changed the position of the nucleation point, keeping the double-asperity seismic moment distribution. In the first example, with the rupture propagating eastwards, the distribution of velocities has one broad lobe directed eastwards, with a maximum velocity value of 80 cm/s near Tarvisio city (Fig. 7, left side). This scenario does explain part of the damages occurred in Austria (velocity values  $\sim 20$  cm/s) and in Slovenia, but not the damage occurred in Friuli Venezia Giulia.

In the case of the westward rupture propagation (Fig. 7, right side), the situation is quite different, with a two-lobes distribution towards SW and NW, with the latter lobe broader with respect to the other one (see the 20 cm/s isoline). The maximum value of the horizontal velocity seems again to be  $\sim 80$  cm/s, but located in Slovenia. This scenario does explain part of the damages occurred in Austria (velocity values between 10 cm/s and 20 cm/s) and in Friuli Venezia Giulia (velocity values  $\sim 20$  cm/s near Venzone and Gemona), but not so well as the first scenario with a bilateral rupture.

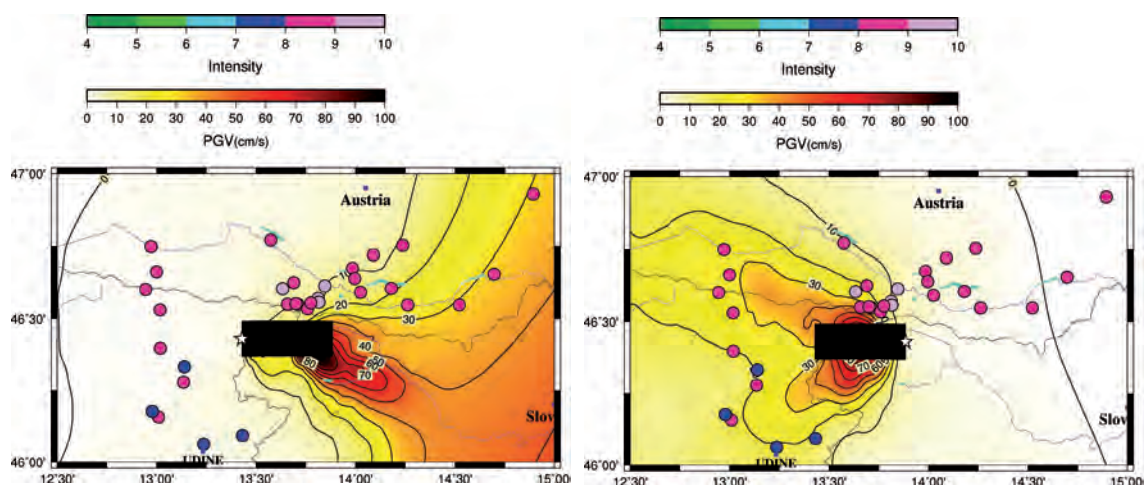


Fig. 7 - Villach 1348 event, unilateral rupture, double asperity seismic moment distribution. The scenarios are superimposed on the observed intensity values (from CPTI11). The black rectangle and the white star are the surface projections of the fault and of the nucleation point, respectively. Left: scenario for the fault rupturing eastwards Right: scenario for the fault rupturing westwards.

### 3.1.3. Comparison with the observed intensity data-points

From a qualitative comparison between our scenarios and the intensity data-points for this specific event (Figs. 6 and 7), taken from both CPTI11 (Rovida *et al.*, 2011) and from Hammerl (1992), the latter including also data from Slovenia, the best agreement between the observed intensities and the ground-shaking scenario seems to be achieved when we consider the scenario with the bilateral rupture using a uniform seismic moment distribution. In fact, this scenario best explains the maximum intensity points both to the north, SE and to the west and SW of the fault.

### 3.2. Idrija 1511 event

The historical earthquake occurred on March 26, 1511, takes its name from a Slovenian city, Idrija, known for its mercury mine and located about 40 km NE from Trieste. Even if this event is rather well studied (e.g., Ambraseys, 1976; Ribarič, 1979; Cergol and Slejko, 1991; Caracciolo and Camassi, 2005; Fitzko *et al.*, 2005; Camassi *et al.*, 2011; Košir and Cecić, 2011), its epicentre is still under debate since estimated from macroseismic data that are still being collected from archives and analysed.

On the other hand, the question about the main event being composed of one or two shocks, was recently solved. The existence of two shocks was due to the wrong interpretation of the available historical information. A unique shock occurred between 3:00 p.m. and 4:00 p.m. of March 26, 1511 (Košir and Cecić, 2011).

As far as the location is concerned, previous authors (e.g., Ambraseys, 1976; Cergol and Slejko, 1991) put the event in the proximity of Mount Matajur, near the border between Italy and Slovenia. Caracciolo and Camassi (2005) shift the location about 18 km towards SW with respect to the previous one proposed by Ambraseys (1976), to an area near Tricesimo city in Friuli Venezia Giulia. This location has been determined using only Italian macroseismic data, and not considering the Slovenian ones.

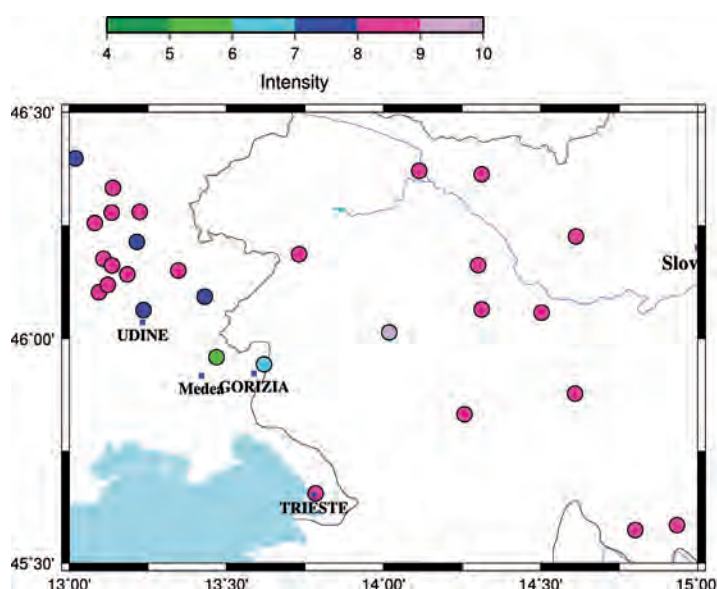


Fig. 8 - Intensity data-points related to the Idrija 1511 event (from CPTI11).

On the contrary Fitzko *et al.* (2005), modeling Italian and Slovenian data and using an extended-fault model, propose as the earthquake causative fault the Idrija one, with a length of 50 km, the rupture propagating towards NW and with the nucleation point located SE of Idrija. In a more recent paper (Camassi *et al.*, 2011) the same authors seem to be more careful about the generating fault of this event, considering also Slovenian macrosismic data (Cecić, personal communication). In our opinion, the modelization of Fitzko *et al.* (2005) seems to be more convincing, but in this paper we produce scenarios based on both the Caracciolo and Camassi (2005) proposal and the Fitzko *et al.* (2005) one. We report in Fig. 8 the map of the intensity data-points from the CPTI11 (Rovida *et al.*, 2011) catalog. The maximum value of the intensity is located near the city of Idrija, but high values of intensities have been proposed also in Friuli Venezia Giulia.

### 3.2.1. Idrija 1511 event: Caracciolo and Camassi (2005) proposal

The fundamental problem we have faced is the selection of the possible generating fault associated with the Caracciolo and Camassi (2005) epicentre. An Alpine thrust fault oriented E-W, or a Dinaric fault oriented SE-NW? We have chosen the Dinaric strike-slip one known either as Raša - Cividale (e.g., Aoudia *et al.*, 2000) or Tricesimo - Cividale fault (Ponton, 2010), which dips towards NE. The source parameters are described in Table 1. Also in this case the slip complexity on the fault was reproduced using a double asperity moment distribution.

#### 3.2.1.1. Bilateral rupture

The ground shaking scenario for a bilateral rupture (Fig. 9) shows an area of strong shaking in the NW direction along the fault strike. The zone characterized by the highest horizontal velocities ( $\sim 100$  cm/s) is located partly above the NW portion of the fault. The isoline of 50 cm/s velocity includes Tarcento - Cividale. This modeling, and also the one using a uniform

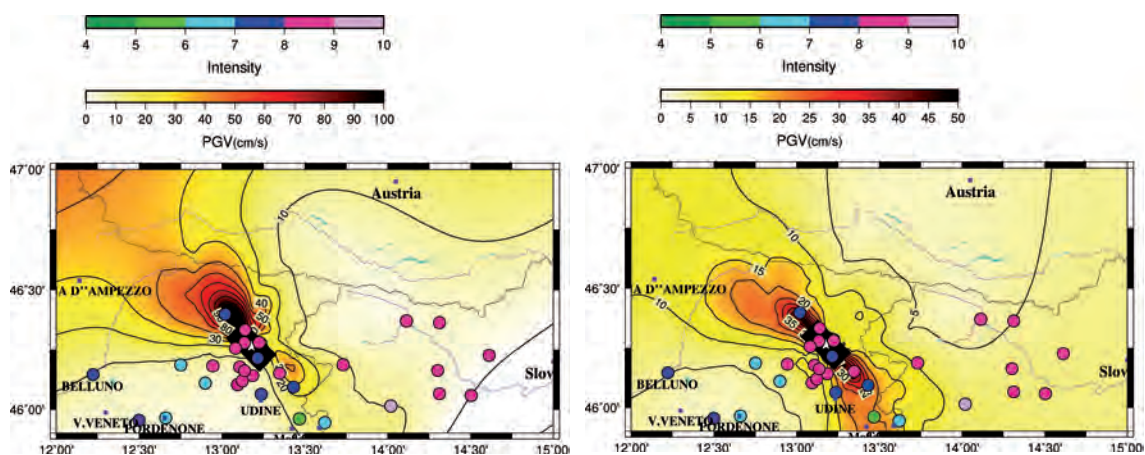


Fig. 9 - Idrija 1511 event, Tricesimo-Cividale fault, bilateral rupture. The scenarios are superimposed on the observed intensity values (from CPTI11). The black rectangle and the white star are the surface projections of the fault and of the nucleation point, respectively. Left: scenario with a double-asperity seismic moment distribution. Right: scenario with a uniform seismic moment distribution.

seismic moment distribution, might well explain the damages in Friuli Venezia Giulia, but not the ones in Slovenia (Camassi *et al.*, 2011).

### 3.2.1.2. Unilateral ruptures

A unilateral rupture model propagating towards NW, produces a single-lobe distribution of ground velocities located NW of the fault (Fig. 10). The maximum computed velocity value is ~110 cm/s. According to this scenario only damages in the northern part of Friuli Venezia Giulia (area with velocities between 40 cm/s and 50 cm/s) can be expected, and no damage in Udine and in the south-eastern part of this region is foreseen (velocity values are not relevant there).

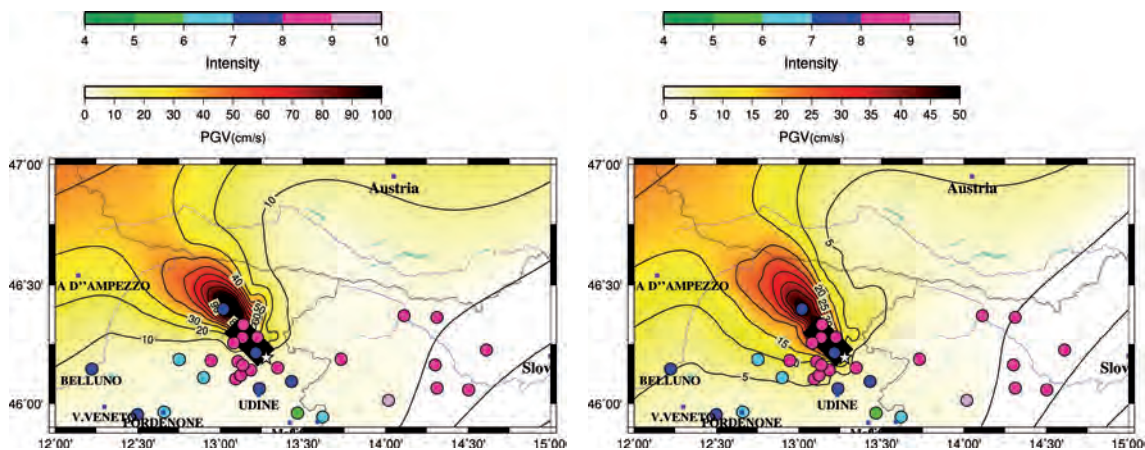


Fig. 10 - Idrija 1511 event, Tricesimo-Cividale fault, unilateral NW-propagating rupture. The scenarios are superimposed on the observed intensity values (from CPTI11). The black rectangle and the white star are the surface projections of the fault and of the nucleation point, respectively. Left: scenario with a double-asperity seismic moment distribution. Right: scenario with a uniform seismic moment distribution.

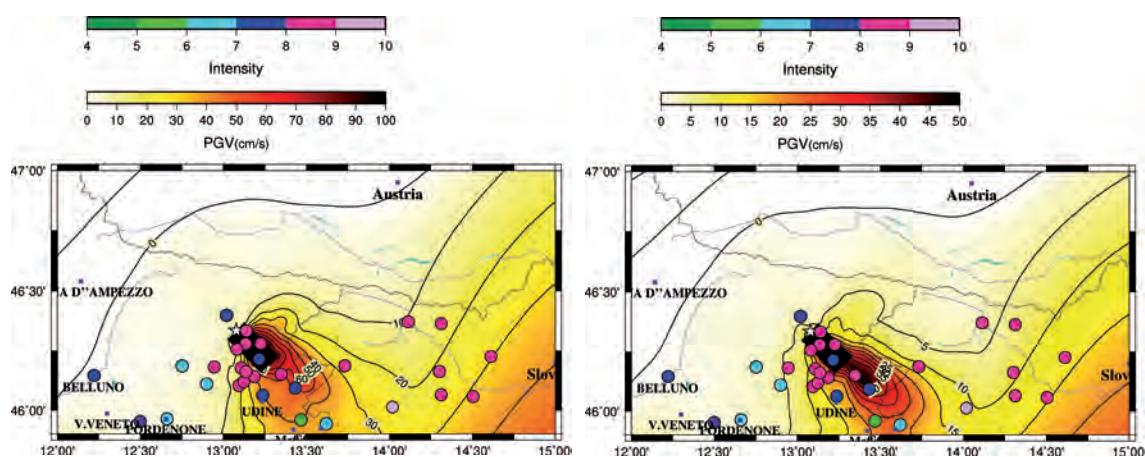


Fig. 11 - Idrija 1511 event, Tricesimo-Cividale fault, unilateral SE-propagating rupture. The scenarios are superimposed on the observed intensity values (from CPTI11). The black rectangle and the white star are the surface projections of the fault and of the nucleation point, respectively. Left: scenario with a double-asperity seismic moment distribution. Right: scenario with a uniform seismic moment distribution.

Moreover, this scenario does not account at all for the damages in Slovenia, as in the case of a uniform seismic moment distribution (Fig. 10, right side).

By placing the position of the nucleation point at the NW edge of the fault we have calculated also a unilateral rupture scenario with the rupture propagating towards SE, but the picture remains basically similar, both when assuming a double asperity distribution or a uniform seismic moment distribution. The main difference is that the velocity distribution has now one lobe towards SE with a maximum velocity value of 100 cm/s located near Tarcento (Fig. 11, left side). This scenario does not explain the damages occurred in Gemona and Venzone (Friuli Venezia Giulia) nor those occurred in Slovenia.

A qualitative comparison of the intensity data-points taken from CPTI11 (Rovida *et al.*, 2011) for this event (Fig. 11, right side) with all three distributions of velocity values calculated using the Tricesimo - Cividale fault as the causative one (Caracciolo and Camassi, 2005) shows that none of the calculated scenarios is able to explain all the observed damages, particularly not the intensity felt in Idrija.

### 3.2.2. Idrija 1511 event: Fitzko *et al.* (2005) proposal

We next investigate the Idrija event using the Fitzko *et al.* (2005) proposal, which assumes that the generating fault is the Idrija one (Table 1). The complexity of the slip on the fault, was reproduced also in this case using a double asperity  $k^2$  (Herrero and Bernard, 1994) moment distribution.

**Bilateral rupture.** The scenario for a bilateral rupture using the Idrija fault, assuming a double-asperity seismic moment distribution with the strongest asperity on its NW part, shows an area with strong ground shaking directed NW (Fig. 12, left part), where the highest horizontal velocity values are  $\sim 60$  cm/s. This scenario explains very well the highest intensity data-point in Idrija, but not the damages occurred in Slovenia. In the case of the uniform seismic moment distribution (Fig. 12, right side) the isoline of 30 cm/s, which includes Tarcento, Cividale to the SE and Gemona, Tolmezzo to the NW. Udine and Gorizia, has a velocity value that is not compatible with the intensities observed in these two cities. Thus, the distribution of  $PGVIHZ$

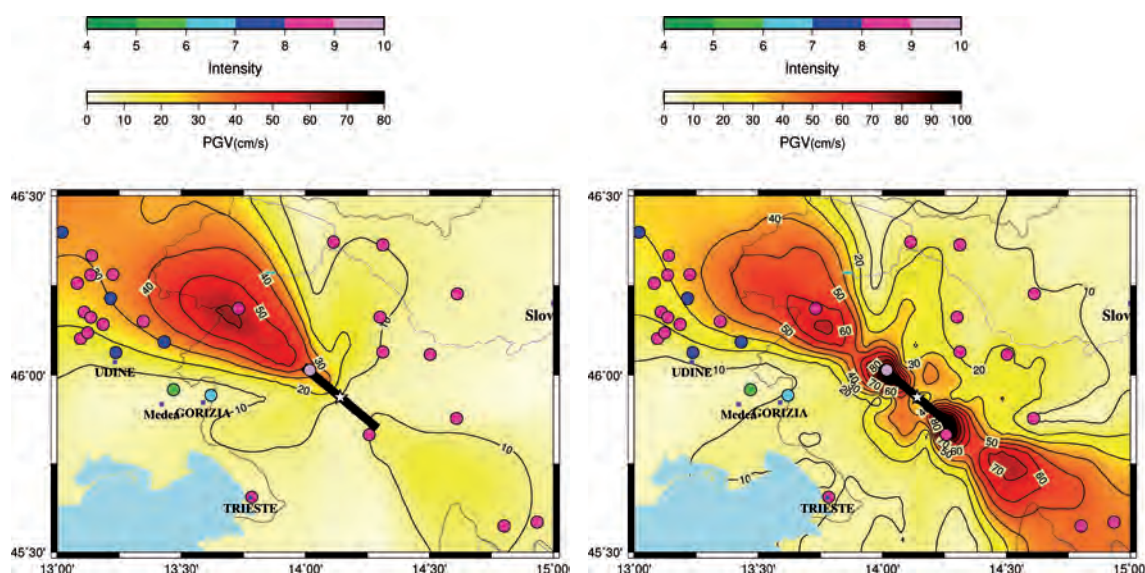


Fig. 12 - Idrija 1511 event, Idrija fault, bilateral rupture. The scenarios are superimposed on the observed intensity values (from CPTI11). The black rectangle and the white star are the surface projections of the fault and of the nucleation point, respectively. Left: scenario with a double-asperity seismic moment distribution. Right: scenario with a uniform seismic moment distribution.

values obtained from this scenario explains very well the damages occurred in Slovenia, but not as well the ones occurred in Friuli Venezia Giulia.

**Unilateral rupture.** The scenarios with the unilateral ruptures, especially the one using a uniform seismic moment distribution (Fig. 13) propagating towards NW, seem to better explain all the intensity data-points related to this event, both the maximum intensity experienced in Idrija, and the damages occurred in Friuli. This scenario is therefore our preferred one for the 1511 earthquake and compatible with the results of Fitzko *et al.* (2005).

### 3.3. Asolo 1695 event

Another historical event studied during the HAREIA project is the Asolo event of February 25, 1695. We have assumed, following Burrato *et al.* (2008), that the generating fault of this event is the Bassano - Cornuda one (Table 1). Due to the considerable fault dimensions, the chosen seismic moment distribution on the fault has two asperities. The intensity data-points, taken from the CPTI11 (Rovida *et al.*, 2011) catalogue, are reported in Fig. 14.

#### 3.3.1. Bilateral and unilateral ruptures

The distribution of interpolated  $PGVIH_z$  values, obtained from the computation of the three usual scenarios based on the Bassano - Cornuda fault, are reported in Fig. 15 for the bilateral rupture, and in Figs. 16 and 17 for the two unilateral ones.

#### 3.3.2. Comparison with the observed intensity data-points

From a qualitative comparison between our three scenarios (in terms of  $PGVIH_z$  values) and the intensity data-points for this event (Fig. 14) taken from CPTI11 (Rovida *et al.*, 2011), the

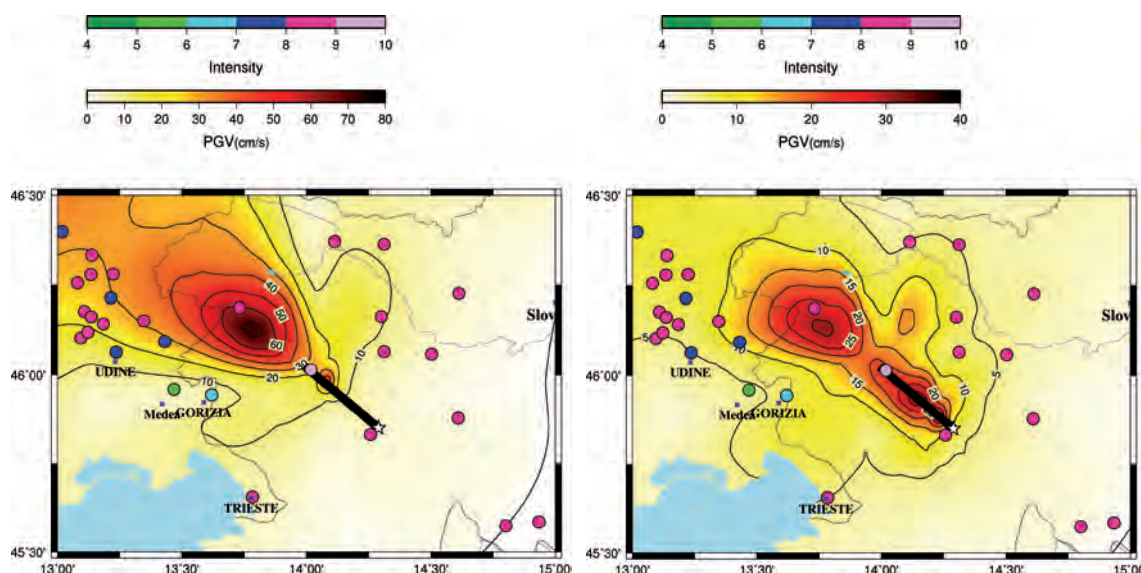


Fig. 13 - Idrija 1511 event, Idrija fault, NW-propagating rupture. The scenarios are superimposed on the observed intensity values (from CPTI11). The black rectangle and the white star are the surface projections of the fault and of the nucleation point, respectively. Left: scenario with a double-asperity seismic moment distribution. Right: scenario with a uniform seismic moment distribution.

attenuation with distance of the computed  $PGV_{1Hz}$  values, that is most similar to the attenuation of the intensity data-points, is the one related to the unilateral rupture propagating towards NE, especially the  $PGV_{1Hz}$  distribution calculated using a uniform seismic moment distribution (see Fig. 16, right side). Also the position of the maximum observed intensity values overlaps with the position of the maximum calculated  $PGV_{1Hz}$  values.

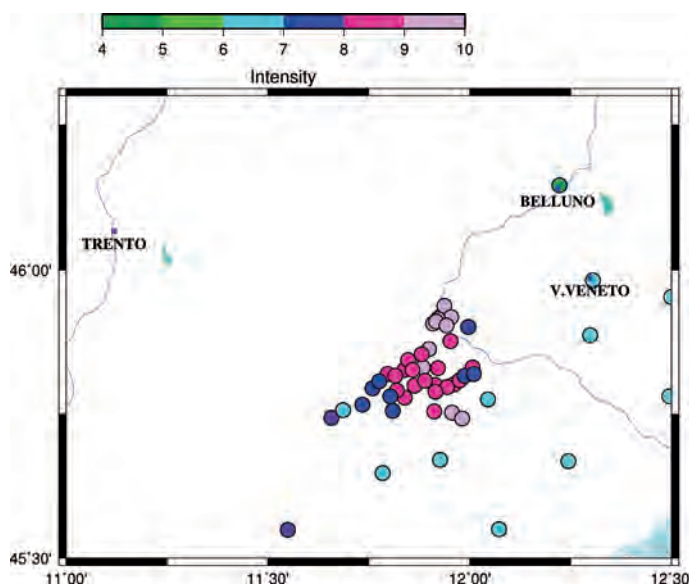


Fig. 14 - Intensity data-points of the Asolo 1695 event (CPTI11).

### 3.4. Tyrol 1572, 1670 and 1689 earthquakes

In the framework of the HAREIA project several events that occurred in Tyrol have been analyzed in terms of their effects/intensities deduced from a critical analysis of archive documents (Hammerl *et al.*, 2012). In particular, the three analyzed events are: the January 4,

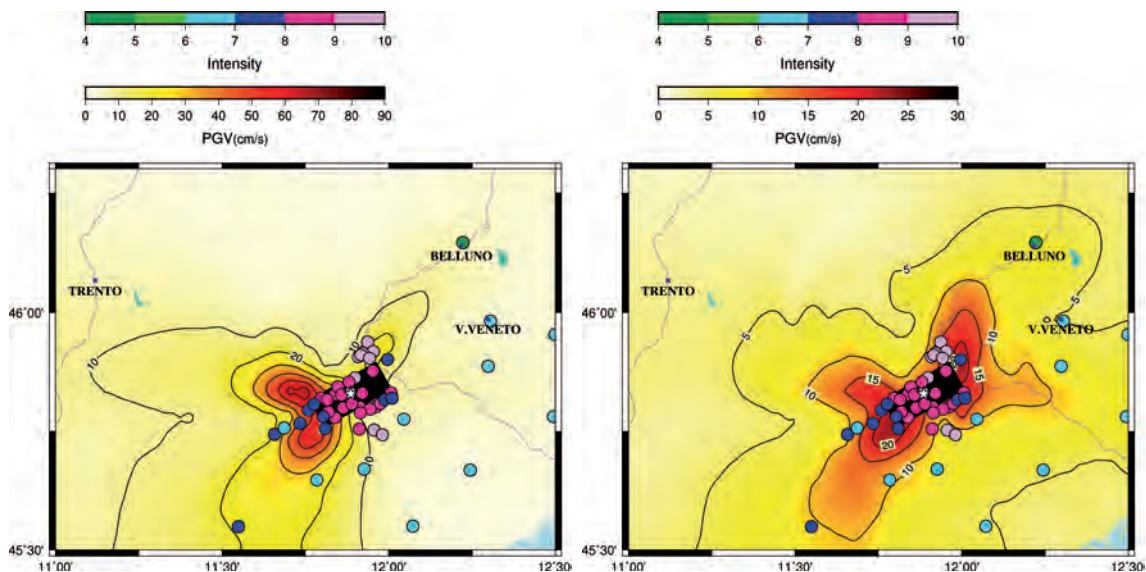


Fig. 15 - Asolo 1695 event, bilateral rupture. The scenarios are superimposed on the observed intensity values (from CPT111). The black rectangle and the white star are the surface projections of the fault and of the nucleation point, respectively. Left: scenario with a double-asperity seismic moment distribution. Right: scenario with a uniform seismic moment distribution.

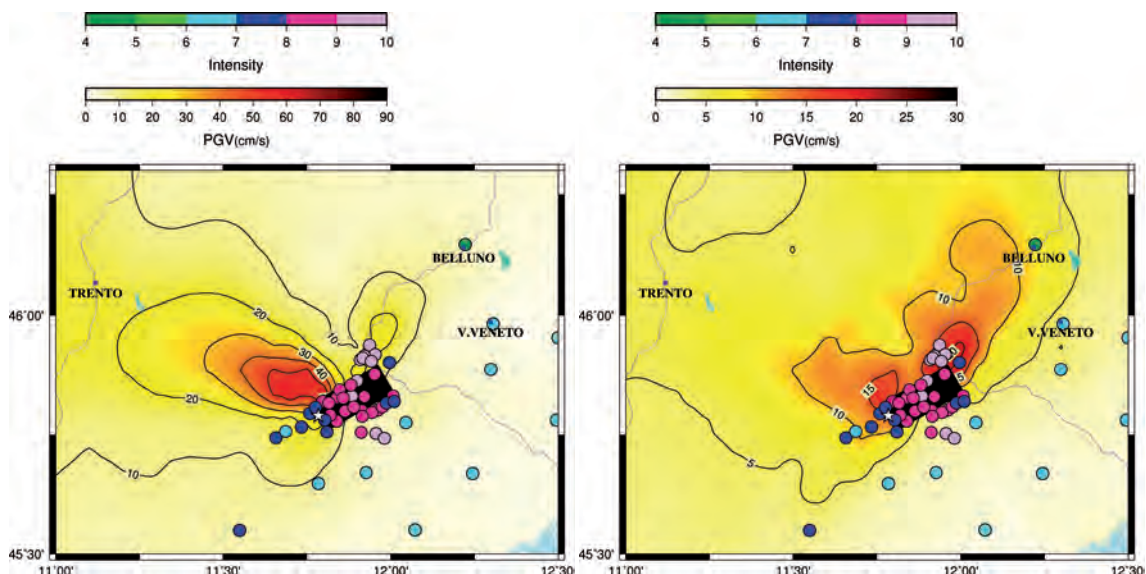


Fig. 16 - Asolo 1695 event, NE-ward propagating rupture. The scenarios are superimposed on the observed intensity values (from CPT111). The black rectangle and the white star are the surface projections of the fault and of the nucleation point, respectively. Left: scenario with a double-asperity seismic moment distribution. Right: scenario with a uniform seismic moment distribution.

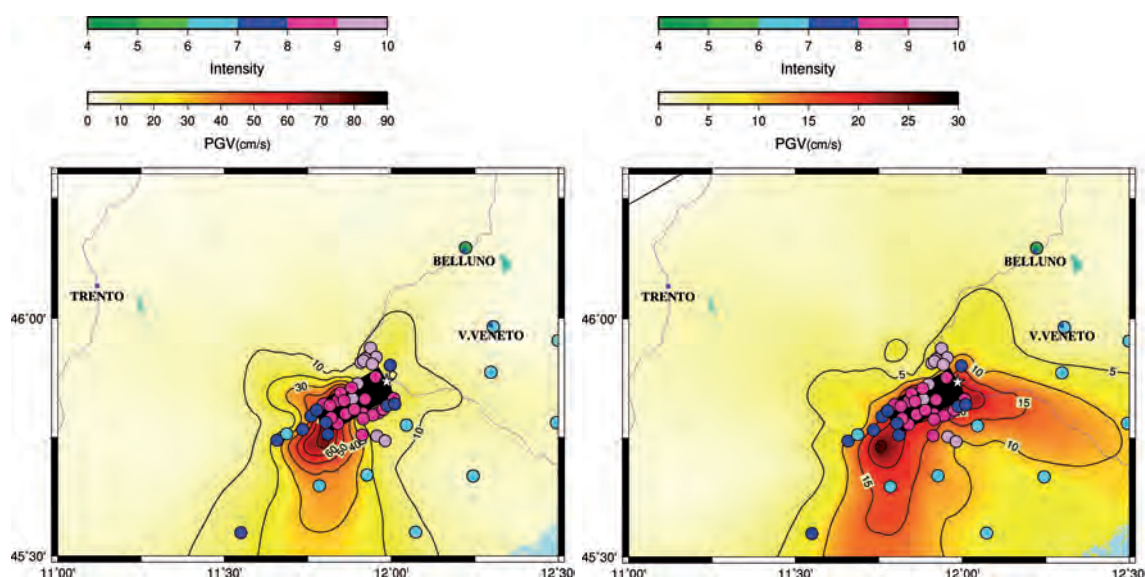


Fig. 17 - Asolo 1695 event, SW-ward propagating rupture. The scenarios are superimposed on the observed intensity values (from CPT111). The black rectangle and the white star are the surface projections of the fault and of the nucleation point, respectively. Left: scenario with a double-asperity seismic moment distribution. Right: scenario with a uniform seismic moment distribution.

1572 in Innsbruck; the July 17, 1670 in Hall, and the December 22, 1689 in Innsbruck. The information obtained in this study relates the intensity data-points of each earthquake to a tentative location and an estimation of its moment magnitude.

Before computing the scenarios for these three events, we have analyzed the seismicity and the known faults of the zone (Reiter *et al.*, 2005). From the map of the area (Fig. 18) we have selected three segments of active faults that could have generated the investigated earthquakes: the Unterinntal Fault Zone (UFZ), the northern part and the central part of the Brenner Normal Fault (BNF). To each segment we have associated a focal mechanism (Table 1). In order to select the best scenario ( $PGVIH_z$  distribution) matching the observed intensity pattern among those related to the three segments, we have qualitatively compared the attenuation with distance from the epicentre of both observed intensities and  $PGVIH_z$  values.

#### 3.4.1. Innsbruck January 4, 1572

This event is modelled with the source parameters reported in Table 1. The intensity data-points (Hammerl *et al.*, 2012) are the ones shown in Fig. 19.

There are only six intensity data-points and they might not be sufficient to discriminate between possible causative faults. The comparison between the intensity values with the related  $PGVIH_z$  values calculated using one of the three selected faults as seismic source (Figs. 19 and 20), provides, however, an indication on the fault we should use for the modelling.

In fact, from a qualitative comparison between all the computed  $PGVIH_z$  distributions and the intensity data-points, the best match seems to be the one computed using as causative fault the northern part of the BNF. Due to the small magnitudes of these events and consequently small fault dimensions, we could not discriminate among various rupture propagations, therefore only the scenario related to the bilateral one is reported (Fig. 21).

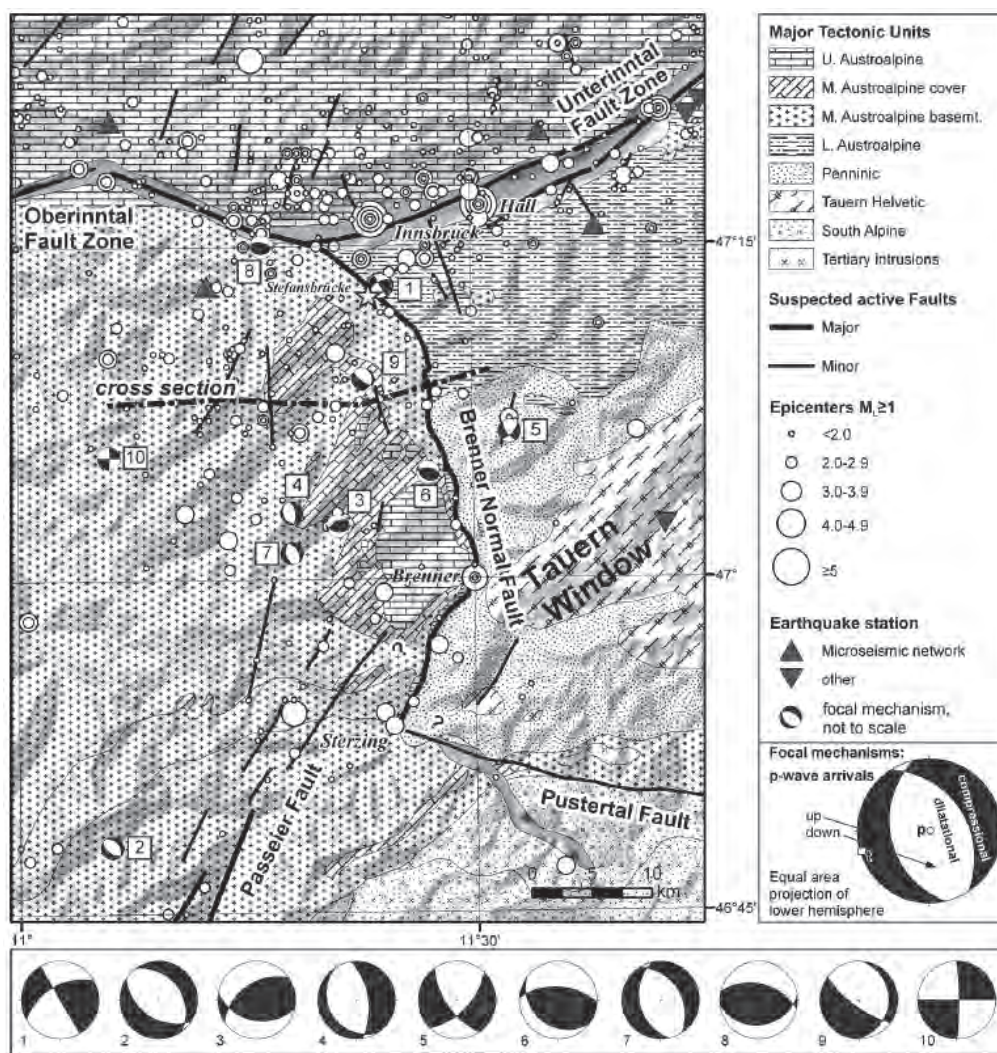


Fig. 18 - Possible causative faults of the three Tyrol events (adapted after Reiter *et al.*, 2005).

### 3.4.2. Hall in Tyrol, July 17, 1670

This event is modelled with the source parameters reported in Table 1. The reported intensity data-points (Hammerl *et al.*, 2012) are shown on the left side of Fig. 22. Also shown is the distribution of  $PGVIH_z$  values for each analyzed fault: UFZ (Fig. 22, right side), the central part of the BNF (Fig. 23, left side), and the northern part of the BNF (Fig. 23, right side).

The obtained results are similar to the ones for the Innsbruck 1572 event. The qualitative comparison clearly shows that the distribution of  $PGVIH_z$  values which best reproduces the pattern of the intensity data-points is the one calculated using the northern part of the BNF. Therefore, we have calculated possible scenarios using only this fault as seismic source (Fig. 24).

As in the previous case, the small fault dimensions prevent us from discriminating the style of rupturing, since the distributions of velocity values are not very sensitive to different nucleation point positions.

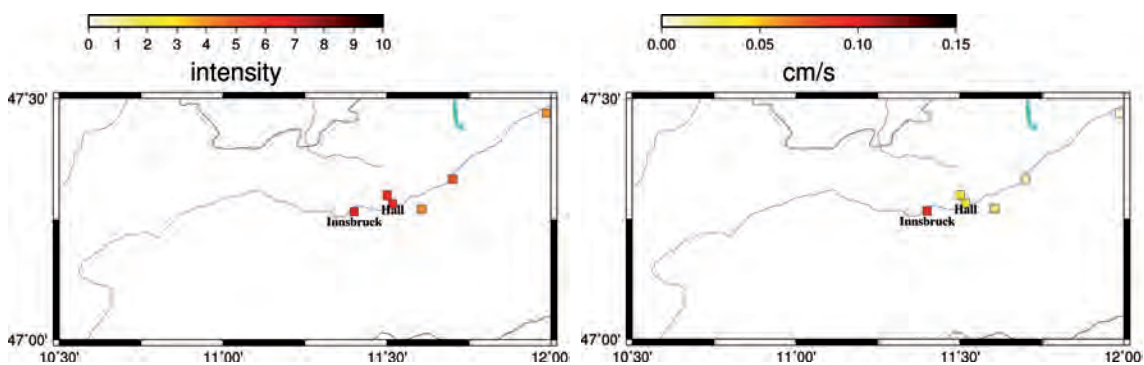


Fig. 19 - Left: intensity data-points of the Innsbruck 1572 event. Right:  $PGV1Hz$  values obtained using the UFZ (Fig. 18) as the causative seismic source.

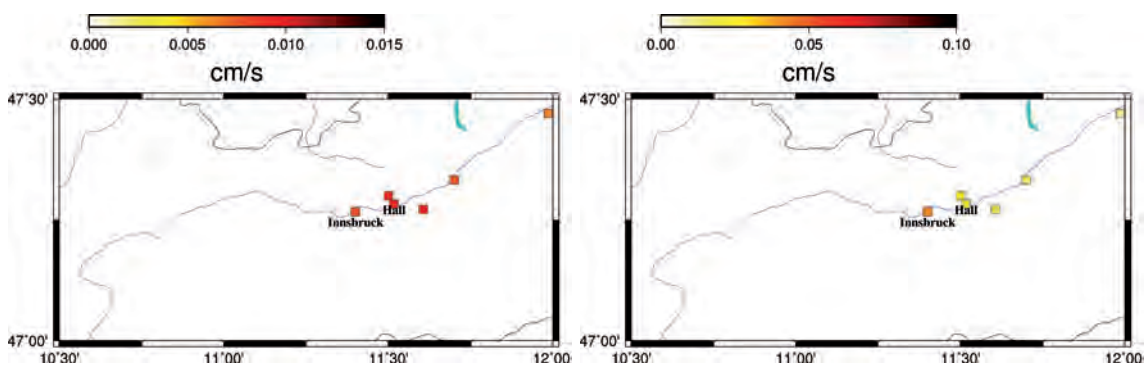


Fig. 20 -  $PGV1Hz$  values obtained using as source part of the BNF. Left: its central part. Right: its northern part.

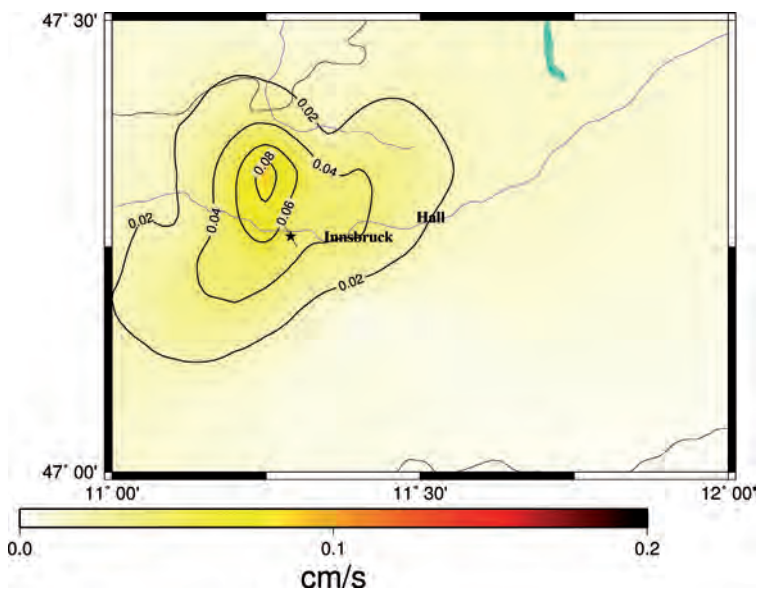


Fig. 21 - Tyrol event of 1572. The scenario for a bilateral rupture using the northern part of the BNF with a uniform seismic moment distribution.

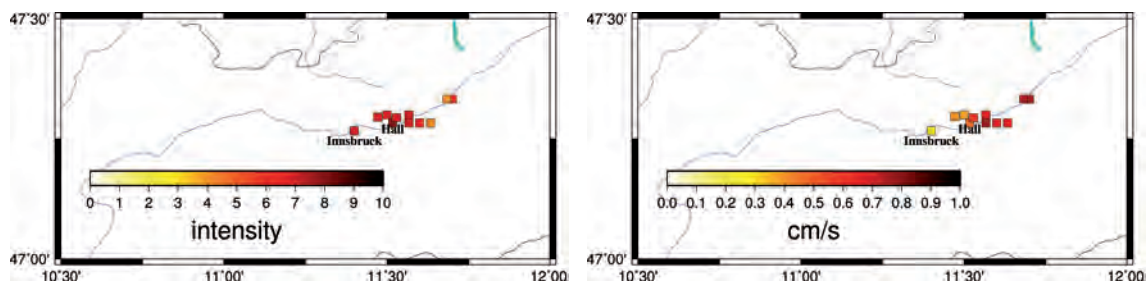


Fig. 22 - Left: intensity data-points of the Hall 1670 event. Right:  $PGVIHz$  values obtained using as source the Unterinntal fault.

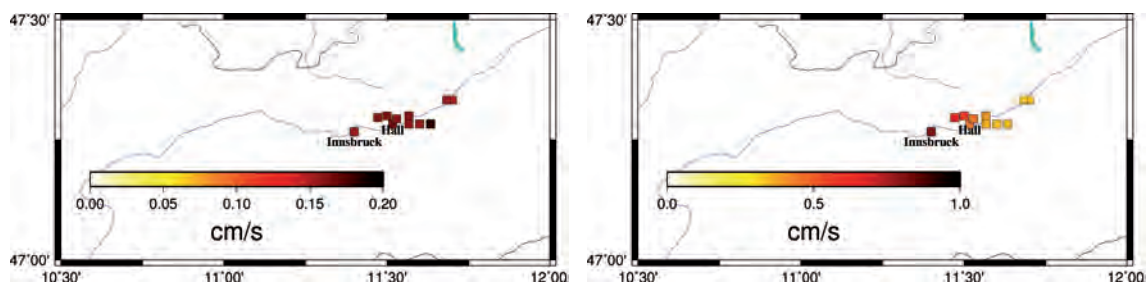


Fig. 23 -  $PGVIHz$  values obtained using as source part of the BNF. Left: its central part. Right: its northern part.

### 3.4.3. Innsbruck, December 22, 1689

The source parameters with which this event is modelled are reported in Table 1. The intensity data-points associated to it are reported in Fig. 25. In the following we report the distribution of the  $PGVIHz$  values computed for each analyzed fault, the UFZ (Fig. 25, right side), the central part of the BNF (Fig. 26, left side), and the northern part of the BNF (Fig. 26, right side).

The  $PGVIHz$  values which best match the intensity data-points are, also in this case, the ones calculated using the northern part of the BNF. So we have calculated the scenarios using this part as the generating fault (Fig. 27). Also this event has a small magnitude and small fault dimensions, which prevent us from discriminating the style of rupturing.

## 4. Conclusions

In the framework of the HAREIA project we have received updated information on the damage and related intensity estimates obtained from a critical analysis of historical documents for the following earthquakes: Villach 1348, Friuli/Idrija 1511, Asolo 1695, from our INGV partners (Caracciolo and Camassi, 2005; Camassi *et al.*, 2011) and Tyrol 1572, 1670 and 1689 events from our ZAMG partners (Hammerl *et al.*, 2012).

In agreement with the epicentral coordinates proposed by our project partners, the extended-source parameters have been deduced from either geological maps of the area of interest or from the literature (e.g., Burrato *et al.*, 2008) and used to produce ground-shaking scenarios for each studied event.

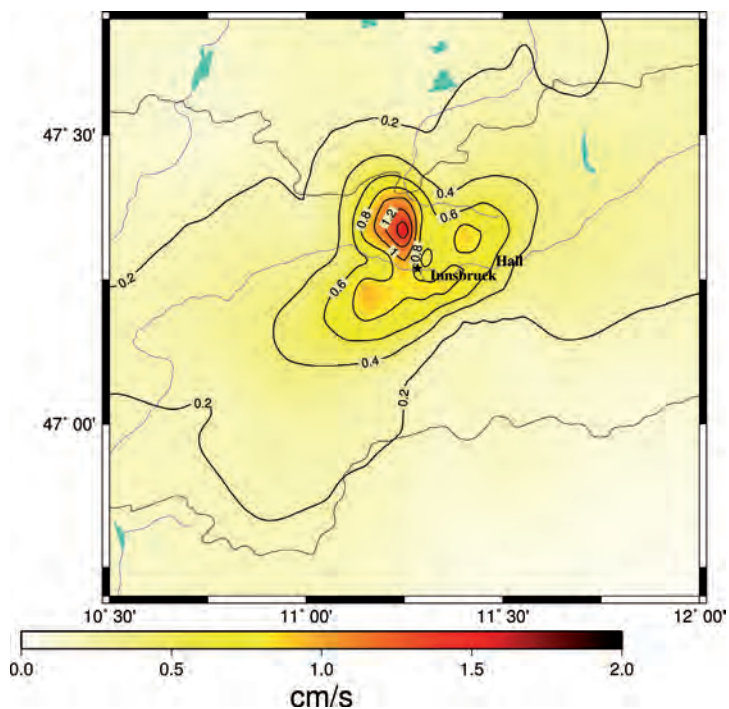


Fig. 24 - Tyrol 1670 event. Scenario for a bilateral rupture with a uniform seismic moment distribution. The northern part of the BNF is considered as the causative fault.

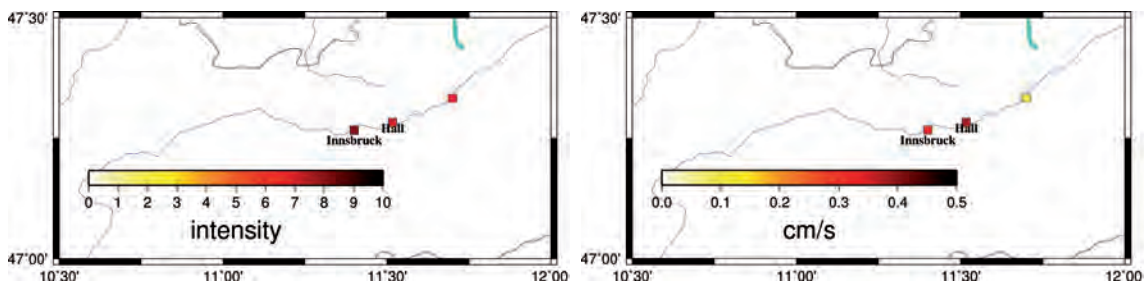


Fig. 25 - Left: intensity data-points of the Innsbruck event of 1689. Right:  $PGVIH_z$  values computed using the UFZ.

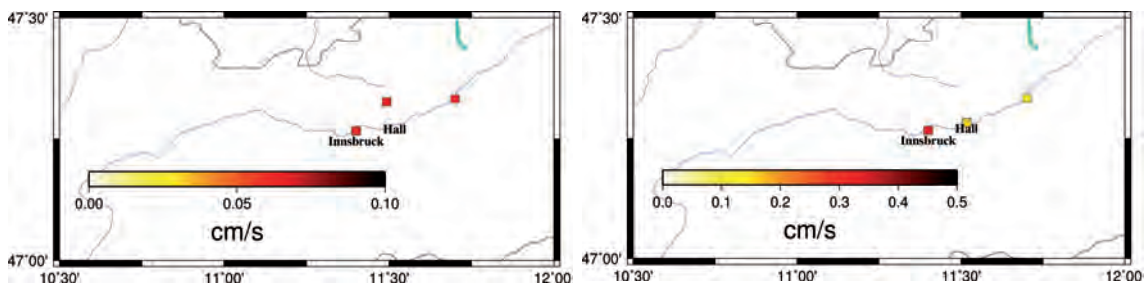


Fig. 26 -  $PGVIH_z$  values computed using as source part of the BNF. Left: its central part. Right: its northern part.

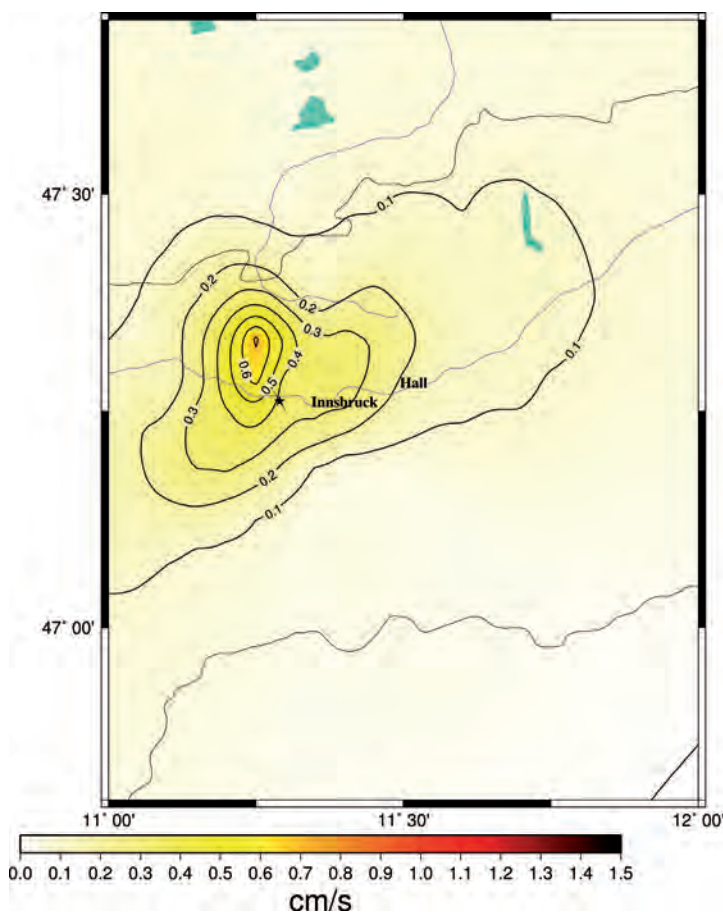


Fig. 27 - Tyrol 1689 event. Scenario for a bilateral rupture with a uniform seismic moment distribution. The northern part of the BNF is considered as the causative fault.

The qualitative comparison between the pattern of intensity data-points and the pattern of  $PGVIH_z$  values obtained from our computed scenarios, leads to the following conclusions. The causative fault of the Villach 1348 event is the Fella - Sava fault with a bilateral rupture. The analysis made for the Idrija 1511 event seems to point out that the better solution is the one proposed by Fitzko *et al.* (2005), with a unilateral rupture on the Idrija fault propagating towards NW. The three Tyrol events are very likely to have been generated by the northern branch of the BNF.

We have extended our analysis to other historical events in order to cover the entire HAREIA project area (Table 2), even if we do not discuss here in detail the related results. In particular, we have studied the sources of Bovec, Cansiglio, Gemona, Maniago, Medea, Merano, Montello, Salò, Sequals, Thiene - Bassano and Tramonti. For each event we have produced several scenarios in terms of  $PGVIH_z$ , changing the rupturing direction and the seismic moment distribution on the fault, according to what has been done and described for the HAREIA events. The overall scenario for the whole HAREIA study area has been computed by taking for each point of the grid covering the area the maximum peak velocity value among the scenarios computed for all analyzed earthquakes, all mechanisms and all rupture models (Fig. 28). One

Table 2 - Source parameters of the other events studied in order the cover with maximum *PGVIH<sub>z</sub>* values the entire area of interest.

Event	Date	Mw	Mo (Nxm)	Epicentral coordinates	Rake	Strike	Dip	Top of the fault (km)	Dimensions of the fault LxW (km)
Bovec	Apr 12, 1998	5.8	$5.0 \times 10^{17}$	46.32°N, 13.61°E	171°	313°	82°	3	13 x 7
Cansiglio	Oct 13, 1936	6.1	$1.4 \times 10^{18}$	45.98°N, 12.41°E	60°	214°	50°	3	10 x 7
Gemona	May 6, 1976	6.4	$3.9 \times 10^{18}$	46.24°N, 13.03°E	105°	290°	30°	3	16 x 9
Maniago	Jul 10, 1776	5.9	$7.0 \times 10^{17}$	46.17°N, 12.67°E	90°	237°	30°	3	8 x 5
Medea	1279?	6.4	$3.9 \times 10^{18}$	45.96°N, 12.67°E	120°	285°	45°	3	16 x 9
Merano	Jul 17, 2001	4.8	$1.6 \times 10^{16}$	46.70°N, 11.16°E	7°	210°	72°	3	3 x 2
Montello	Unknown	6.7	$1.1 \times 10^{19}$	45.88°N, 12.31°E	80°	40°	242°	3	22 x 11
Salò	Oct 31, 1901	5.7	$1.8 \times 10^{17}$	45.58°N, 10.50°E	92°	235°	25°	3	4 x 6
Sequals	Assumed	6.5	$5.6 \times 10^{18}$	46.15°N, 12.77°E	90°	254°	40°	3	16 x 9
Thiene - Bassano	Assumed	6.6	$7.9 \times 10^{18}$	45.69°N, 11.54°E	80°	244°	30°	3	18 x 9
Tramonti	June 7, 1794	5.8	$5.0 \times 10^{17}$	46.27°N, 12.77°E	90°	268°	35°	3	6 x 5

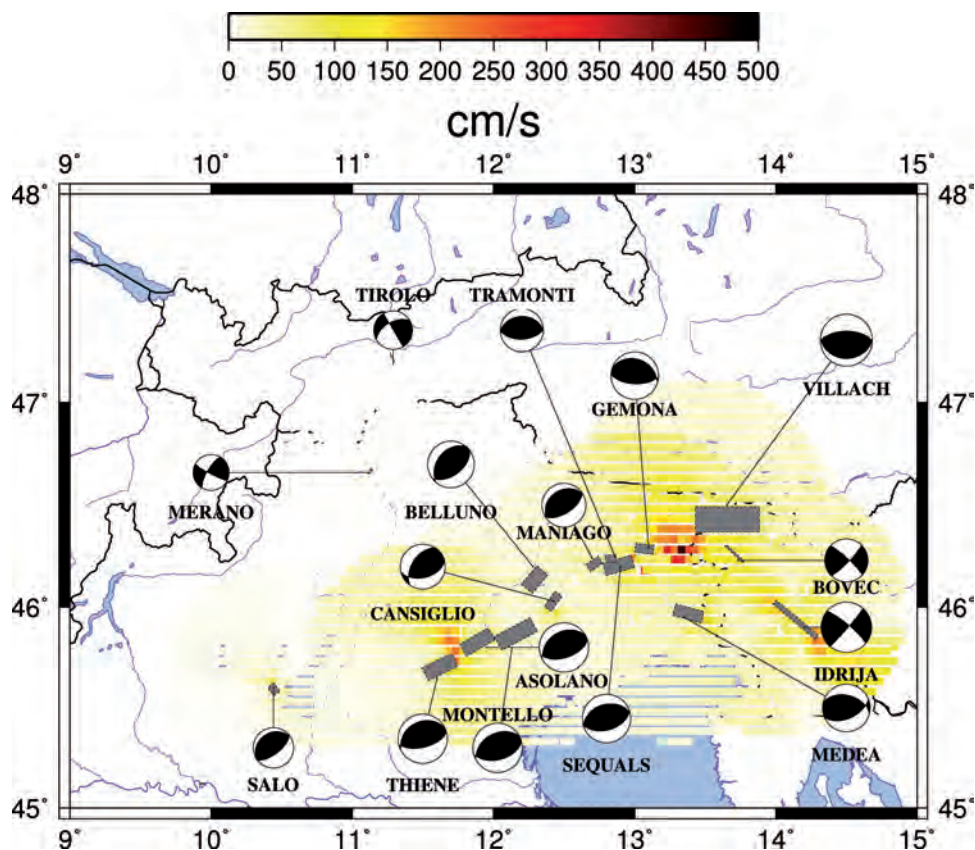


Fig. 28 - Total maximized *PGVIH<sub>z</sub>* distribution for the entire HAREIA project area. The map shows the fault surface projections of the studied earthquakes and their associated focal mechanisms.

can see that most of the events have produced irrelevant values of  $PGVIH_z$ . The maximum computed velocity values, up to about 500 cm/s, are those related to the Gemona and to the Thiene - Bassano events.

The Gemona event occurred on May 6, 1976 and mostly damaged the areas near Gemona, Venzone and Tolmezzo. The maximum value of  $PGVIH_z$  calculated for this event is  $\sim 500$  cm/s. The Thiene - Bassano event is not associated to a specific historical earthquake, and we have decided to model it because the Thiene - Bassano thrust fault activity is documented by numerous geological studies (e.g., Galadini *et al.*, 2005; Burrato *et al.*, 2008). The maximum value of  $PGVIH_z$  calculated for this event is  $\sim 300$  cm/s.

This map could be useful as starting point for future research of earthquake sources in this area, and in particular could be used as a guideline for Civil Defense in order to foster the strengthening of the build environment and thus mitigate possible future disasters in this high-risk seismic area. It can be also used to keep the local communities aware and resilient.

**Acknowledgements.** This research was funded by the Interreg IV HAREIA project. We are grateful to our project partners: INGV, OGS, ZAMG, Civil Defences of Tyrol, South Tyrol and Friuli Venezia Giulia for the help provided within this project. We thank the two anonymous reviewers for their very helpful comments that have helped to improved the paper. This paper was presented at the EGU2012 meeting in Vienna.

## REFERENCES

- Ambraseys N.N.; 1976: *The Gemona Friuli earthquake of 6 May 1976*. In: Pichard P., Ambraseys N.N., Ziogas G.N. (eds), UNESCO Restricted Technical Report, RP/1975-76/2.222.3, Paris II, pp. 1-111
- Aoudia A., Saraò A., Bukchin B. and Suhadolc P.; 2000: *The Friuli 1976 event: a reappraisal 23 years later*. Geophys. Res. Lett., **27**, 573-576.
- Bajc J., Aoudia A., Saraò. A. and Suhadolc P.; 2001: *The 1998 Bovec - Krn mountain (Slovenia) earthquake sequence*. Geophys. Res. Lett., **28**, 1839-1842.
- Burrato P., Poli M.E., Vannoli P., Zanferrari A., Basili R. and Galadini F.; 2008: *Sources of Mw 5+ earthquakes in northeastern Italy and western Slovenia: an updated view based on geological and seismological evidence*. Tectonophys., **453**, 157-176.
- Camassi R., Caracciolo C.H., Castelli V. and Slejko D.; 2011: *The 1511 Eastern Alps earthquakes: a critical update and comparison of existing macroseismic datasets*. J. Seismol., **15**, 191-213, doi:10.1007/s10950-010-9220-9.
- Caracciolo C.H. and Camassi R.; 2005: *Miglioramento delle conoscenze sui terremoti del Friuli*. Rapporto tecnico per INOGS, Bologna, Italy, 21 pp.
- Carulli G.B.; 2006: *Carta geologica del Friuli Venezia Giulia, scala 1:150.000*. Regione Autonoma Friuli Venezia Giulia, S.El.Ca., Firenze, Italy, 44 pp.
- Cergol M. and Slejko D.; 1991: *The Eastern Alps earthquake of March 26, 1511: state-of-the-art*. In: Proc. Third Int. Workshop on Historical Earthquakes in Europe, Liblice by Prague, Czech Republic, pp. 197-211.
- Costa G., Panza G., Suhadolc P. and Vaccari F.; 1992: *Zoning of the Italian region with synthetic seismograms computed with known structural and source information*. In: Proc. Tenth World Conference on Earthquake Engineering, Madrid, Spain, pp. 435-438.
- Fitzko F., Suhadolc P., Aoudia A. and Panza G.F.; 2005: *Constraints on the location and mechanism of the 1511 Western-Slovenia earthquake from active tectonics and modeling of macroseismic data*. Tectonophys., **404**, 77-90.
- Florsch N., Fäh D., Suhadolc P. and Panza G.F.; 1991: *Synthetic seismograms for high-frequency multimode SH-waves*. Pageoph, **136**, 529-560.
- Galadini F., Poli M.E. and Zanferrari A.; 2005: *Seismogenic sources potentially responsible for earthquakes with  $M > 6$  in the eastern Southern Alps (Thiene - Udine sector, NE Italy)*. Geophys. J. Int., **161**, 739-762.

- Gentile F., Renner G., Riggio A.M., Slejko D. and Zacchigna M.; 1985: *The Villach earthquake of January 25, 1348*. In: Postpischl D. (ed), Atlas of isoseismal maps of Italian earthquakes, Quaderni Ricerca Scientifica, **114**, 14-15.
- Gutdeutsch R. and Lenhardt W.; 1996: *Seismological interpretation of the South Alpine earthquake of January 25th, 1348*. In: Thorkelsson B. (ed), Seismology in Europe, XXV General Assembly of European Seismological Commission, Reykjavik, Iceland, pp. 634-638.
- Hammerl Ch.; 1992: *Das Erdbeben vom 25. Jänner 1348 - Rekonstruktion des Naturereignisses*. PhD thesis, University Wien, Wien, Austria, 256 pp.
- Hammerl C.; 1994: *The earthquake of January 25th, 1348: discussion of sources*. In: Albin P. and Moroni A. (eds), Materials of the CEC project "Review of Historical Seismicity in Europe", CNR, Milano, Italy, vol. 2, pp. 225-240.
- Hammerl C., Lenhardt W.A. and Innerkofler M.; 2012: *Historische erdbeben in Tirol. Forschungen im rahmen des INTERREG IV Projektes HAREIA (Historical and recent Earthquakes in Italy and Austria)*. In: Zanesco A. (ed), Forum Hall in Tirol, Neues zur Geschichte der Stadt, Band 3, Innsbruck, Austria, pp. 174-205.
- Heaton T.H.; 1990: *Evidence for and implications of self-healing pulses of slip in earthquake rupture*. Phys. Earth Planet. Inter., **64**, 1-20.
- Herrero A. and Bernard P.; 1994: *A kinematic self-similar rupture process for earthquakes*. Bull. Seismol. Soc. Am., **84**, 1216-1228.
- Košir M. and Cecić I.; 2011: *Potres 26. marca 1511 v luči novih raziskav*. Idrijski razgledi, **56**, 90-104 (in Slovenian with English abstract).
- Moratto L., Costa G. and Suhadolc P.; 2009: *Real-time generation of shake maps in the Southeastern Alps*. Bull. Seismol. Soc. Am., **99**, 2489-2501.
- Panza G.F. and Suhadolc P.; 1987: *Complete strong motion synthetics*. In: Bolt B.A. (ed), Seismic strong motion synthetics, Academic Press, Orlando, FL, USA, pp. 153-204.
- Ponton M.; 2010: *Architettura delle Alpi Friulane*. In: Museo Friulano di Storia Naturale, Pubbl. n. 52, Udine, Italy, pp. 9-69.
- Reiter F., Lenhardt W.A. and Brandner R.; 2005: *Indications for activity of the Brenner Normal Fault Zone (Tyrol, Austria) from seismological and GPS data*. Austrian J. Earth Sci., **97**, 16-23.
- Ribarič V.; 1979: *The Idrija earthquake of March 26, 1511 - a reconstruction of some seismological parameters*. Tectonophys., **53**, 315-324.
- Rovida A., Camassi R., Gasperini P. and Stucchi M. (a cura di); 2011: *CPTIII, la versione 2011 del Catalogo Parametrico dei Terremoti Italiani*. INGV, Milano - Bologna, Italy, 30 pp.
- Sarà A., Das S. and Suhadolc P.; 1998: *Effect of non-uniform station coverage on the inversion for earthquake rupture history for a Haskell-type source model*. J. Seismol., **2**, 1-25.
- Somerville P., Irikura K., Graves R., Sawada S., Wald D., Abrahamson N., Iwasaki Y., Kagawa T., Smith N. and Kowada A.; 1999: *Characterizing crustal earthquake slip models for the prediction of strong ground motion*. Seismol. Res. Lett., **70**, 59-80.
- Wald D.J., Worden B.C., Quitoriano V. and Pankow, K.L.; 2005: *ShakeMap manual: technical manual, user's guide, and software guide*. U.S. Geological Survey, 132 pp.
- Wells D.L. and Coppersmith K.J.; 1994: *New empirical relationships among magnitude, rupture length, rupture width, rupture area and surface displacement*. Bull. Seismol. Soc. Am., **84**, 974-1002.

Corresponding author: Giovanni Costa  
Dipartimento di Matematica e Geoscienze, Università di Trieste  
Via E. Weiss 2, 34128 Trieste, Italy  
Phone: +39 040 5582124; fax: +39 040 5582111; e-mail: costa@units.it